5-2017

Role of Nanoparticles in Voltammetric Signal Enhancement Exhibited by Layer-by-Layer (LbL) Gold Nanoparticle-Modified Screen-Printed Carbon Electrodes (SPCEs)

Ben K. Ahiadu
East Tennessee State University

Role of Nanoparticles in Voltammetric Signal Enhancement Exhibited by Layer-by-Layer (LbL) Gold Nanoparticle-Modified Screen-Printed Carbon Electrodes (SPCEs)

A thesis

presented to

the faculty of the Department of Chemistry

East Tennessee State University

In partial fulfillment

of the requirements for the degree

Master of Science in Chemistry

---

by

Ben Kwasi Ahiadu

May 2017

Dr. Gregory W. Bishop, Chair

Dr. Dane W. Scott

Dr. Marina Roginskaya

Keywords: screen-printed electrodes, voltammetry, layer-by-layer electrostatic adsorption, gold nanoparticles

ABSTRACT

Role of Nanoparticles in Voltammetric Signal Enhancement Exhibited by Layer-by-Layer Gold Nanoparticle-Modified Screen-Printed Carbon Electrodes (SPCEs)

by

Ben Kwasi Ahiadu

Screen-Printed Electrodes (SPEs) have found wide use as sensing platforms due to their simple fabrication, customizability in terms of geometry and composition, and relatively low cost of production. Nanoparticles have been incorporated in or interfaced with SPEs in order to improve sensor response or provide electrocatalytic capabilities. Though nanomaterial-modified SPEs are becoming increasingly common sensing platforms, the benefits provided by nanomaterials are often determined through voltammetric studies with common redox probes, such as ferricyanide. However, recent reports have documented the ferri-/ferrocyanide redox couple to be an unreliable system for characterizing some carbon-based electrodes due to the dependence of its electrochemical response on electrode surface effects unrelated to electroactive surface area. In the current studies, we have investigated the voltammetric responses of ferricyanide and other redox probes on bare and gold nanoparticle (AuNP)-modified screen-printed carbon electrodes to determine the potential role of AuNPs in improving sensor response through electrochemical signal enhancement.

DEDICATION

This work is dedicated to Forgive Agbenyegah, Mr. Vincent Kaledzi, my siblings and my parents.

ACKNOWLEDGEMENTS

I would like to thank God for seeing me through all these years of academic and professional training. This work would not have seen the light of day without the hard work and inspiration from my indefatigable advisor, Dr. Gregory Bishop. I therefore want to express my profound gratitude to Dr. Gregory Bishop for his encouragement and being a resource for me during this research work. My heartfelt gratitude also goes to Dr. Marina Roginskaya and Dr. Dane Scott for their willingness to serve as my thesis advisory committee members, and their roles in bringing me up as a young chemist. I also want to thank Rev. Dr. Arnold Nyarambi for his encouragement and guidance. My sincere appreciation also goes to all my colleagues in Dr. Bishop's research lab, and all professors in the chemistry department. I say God bless you all.

TABLE OF CONTENTS

LIST OF TABLES

LIST OF FIGURES

LIST OF ABBREVIATIONS

CV – Cyclic voltammetric

DMF – N,N-dimethyl formamide

$FcCH_2OH$ – Ferrocenemethanol

GSH-AuNP– Glutathione-capped gold nanoparticles

HOPG – Highly oriented pyrolytic graphite

LbL – Layer-by-Layer

PDDA – Poly(diallyldimethylammonium)

PVA – Polyvinyl acetate

PVC – Polyvinyl chloride

SPCE – Screen-Printed Carbon Electrode

SPE – Screen-Printed Electrode

CHAPTER 1

INTRODUCTION

Biosensors and Biomarkers

There has been an ever-increasing demand for simple, fast, accurate, and low-cost analytical devices, especially in the field of healthcare, where improvements in such tools and platforms can result in more accessible, affordable, and effective diagnoses and treatment strategies.[1] One class of analytical devices that is particularly important to health-related diagnostics is biosensors. Biosensors are analytical devices that make use of biological recognition elements like antibodies, aptamers, or complimentary nucleic acid sequences to capture and quantify biomolecules (e.g. proteins, nucleic acids, metabolites, etc.) present in biological samples (e.g. urine, blood, serum, etc.).[1,2] Such biomolecules that can be objectively measured and are found to be related to disease state or immune response are called biomarkers [3] and can be used to help diagnose and predict disease progression.

In biosensors, the biorecognition event (i.e. capture of biomarker through use of recognition agent) is converted (usually through enzymatic or chemical reaction) to an interpretable analytical signal that is proportional to the amount of the biomarker present in the sample.[4,5] Concentrations of biomarkers in a patient's sample can be used to determine the presence or severity of a disease state in the patient. Detection and quantification of biomarkers can therefore provide information about normal or pathogenic processes, or pharmacological responses to medical interventions.[4]

Electrochemical Biosensors and Screen-Printed Electrodes

Biosensors based on measurement of electrochemical signals, known as electrochemical biosensors, are particularly appealing due to the relatively low cost, ease of operation, and lack of maintenance associated with electrochemical instrumentation.[6] Electrochemical biosensors employ electrodes, usually modified with a recognition agent specific for the analyte (the biomolecule of interest), and the presence of the analyte at the electrode surface is measured through an electrochemical reaction that generates a signal in the form of an electric current or difference in electric potential. A variety of electrochemical strategies for biosensing have been described and continue to be developed, enabling relatively simple design and implementation of systems capable of sensitive measurements required for clinical applications.[5,7]

Screen-printed electrodes (SPEs), which are produced by depositing a mixture of metal or carbon particles and a polymeric binder (i.e. conductive ink or paste) through a stencil onto an insulating polymer or ceramic substrate (Figure 1), have emerged as particularly promising platforms for electrochemical biosensing. Development of SPEs began in the 1990s,[4] and their application as sensing platforms has continued to garner much interest due to their low cost of fabrication, ease of mass production, and ability to be customized through use of different conductive inks, and geometric patterns defining electrode size and placement.[4] Conductive inks and pastes for printing these electrodes are commercially available,[8] and several manufacturers also offer screen-printed electrodes prepared from various inks and sometimes with customizable geometric specifications.[9]

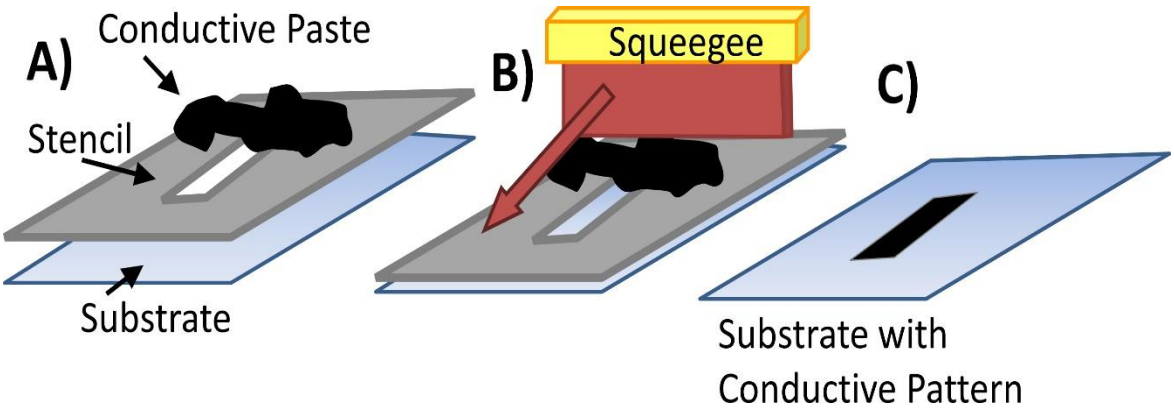

Figure 1:An illustration of the basic manual screen-printing process used to make screen-printed electrodes. A) Conductive paste is deposited on a stencil that features the desired design. B) The stencil is placed on top of the substrate (usually an insulating polymer film or ceramic material) and a squeegee is used to force ink over the surface of the stencil and onto the substrate below. C) The screen-printing process results in the deposition of the conductive paste onto the substrate in a pattern that has been defined by the stencil.

Screen-printed electrodes have been employed in many electrochemical applications, ranging from clinical and environmental analyses,[10,11] to energy conversion and storage devices.[12] For example, screen-printed electrodes have been used in determination of organic pollutants such as hydroquinone and catechol in water samples, and measuring pH.[9] They have also been used as DNA-based electrochemical platforms for patient diagnoses.[13]

The most prominent commercial use of screen-printed electrodes is found in glucose biosensors, which have dominated the $ 5 billion-per-year diabetes monitoring market over the past three decades.[2] The devices consist of glucose oxidase-modified screen-printed electrodes coupled with portable amperometric meters that measure current associated with the enzymatic reaction of glucose with glucose oxidase which generates hydrogen peroxide, an electrochemically active molecule that is involved in many biosensing strategies. The electrochemical signal generated in the course of oxidizing hydrogen peroxide produced from the enzymatic reaction is proportional to the amount of glucose present.[6] Glucose biosensors are compatible with blood sample volumes as small as 0.5- 10 µL, and the resulting signals are

generated within 5- 10 s.[2] However, nanomaterial modified screen-printed electrodes have been investigated as potential replacements for enzyme-modified electrodes due to the relative lack of stability of enzymes.[2,14]

Nanomaterial-Modified Screen-Printed Electrodes.

A growing number of electrochemical sensors are based on screen-printed electrodes modified with or composed of various nanomaterials, including metal nanoparticles, carbon nanotubes, and graphene.[15,16] The intense interest in these nanostructured electrodes stems from their beneficial electrochemical properties such as large surface area-to-volume ratio, improved electron transfer kinetics, and electrocatalytic properties compared to electrodes prepared from bulk materials of similar composition.[2,15] Screen-printed electrodes (SPEs) modified with nanomaterials such as Prussian blue and platinum nanoparticles,[16] as well as those composed of graphene-based conductive ink are commercially available.[10] Such electrodes can also be prepared by incorporating nanomaterials into inks or depositing the nanoparticles onto SPEs through adsorption or electrodeposition.

One simple and effective method of modifying screen-printed electrodes with nanomaterials is known as the layer-by-layer (LbL) technique. [10,17,18] This method, which makes use of electrostatic interactions between layers of oppositely charged materials, has been widely used in modifying and changing the surface functionalities of bulk electrodes.[11,15,17] This technique serves as a fast, simple and effective way of fabricating micro- or nanostructured electrodes. In making sensors and biosensors through LbL method, charged polymers like polystyrene sulfonate, poly(diallyldimethylammonium chloride) (PDDA), phthalocyanine tetrasulfonate, or poly(allylamine hydrochloride) are used[13] to help adsorb oppositely charged semiconductors, enzymes, metallic materials or carbon-based nanomaterials (like nanospheres,

carbon nanotubes, nanorods, or graphene sheets) onto an electrode.[12,19] Nanomaterial-modified electrodes prepared through the LbL technique have been reported to possess improved electrochemical properties including enhanced sensitivity and better electron transfer kinetics, compared to electrodes composed of bulk material analogs.[10,17]

One common way of verifying and quantifying benefits of nanoparticle modification involves comparison of electrochemical signals associated with common redox probes like ferricyanide using bare (unmodified) and nanoparticle-modified electrodes.[7,8,10] Nanoparticle-modified electrodes typically exhibit larger currents attributed to redox probe oxidation or reduction compared to unmodified or bare electrodes. This increase in signal is interpreted as an increase in electroactive surface area, which is the available portion of the working electrode that can participate in the electron transfer. Improvement in electrochemical signal and by extension electroactive surface area is rationalized by the well-documented large surface area-to-volume ratio of nanomaterials compared to bulk materials and thus attributed to the presence of the nanostructures on the electrode surface.[8]

A previous report demonstrated, by using ferricyanide as a redox probe, that the electroactive surface area of screen-printed carbon electrodes (SPCEs) could be increased by 102% by modifying the electrodes with glutathione-capped gold nanoparticles (GSH-AuNPs) through the LbL technique using polycation poly(diallyldimethylammonium) (PDDA).[10] However, recent reports[20,21] involving measurements of ferricyanide response using other carbon-based electrodes have cast doubt on the origin of the electrochemical signal increase that is currently attributed to the effects of the nanomaterials. These studies have basically attributed increases in electrochemical signals and variations in electron transfer kinetics to the surface

sensitivity of ferricyanide rather than the presence of nanomaterials, as results with other redox probes failed to show the same kinds of signal enhancement as those obtained with ferricyanide.

Research Objectives

In this work, the role of nanoparticles in electrochemical signal enhancement is investigated through characterization of bare and LbL-prepared GSH-AuNP-modified SPCEs using cyclic voltammetric responses of common redox couples ferri-/ferrocyanide ($Fe(CN)_6^{3-/4-}$), ferrocene-/ferrocenium methanol ($FcCH_2OH/FcCH_2OH^+$) and hexaammineruthenium(III)/(II) ($Ru(NH_3)_6^{3+/2+}$). The effect of redox probe selection for electrode characterization and function of the polycationic PDDA layer used to adsorb GSH-AuNPs through LbL technique onto the SPCE surface are also addressed. The additional information provided by measurements of multiple redox probes enables more thorough comparison of bare and modified SPCEs in a way that leads to an improved understanding of the effects nanoparticles have on electrochemical signal for these particular LbL-prepared SPCEs. Results here may also extend to other nanomaterial-modified SPEs and carbon-based electrodes as voltammetric response of ferricyanide is a common (and sometimes the only) method employed in comparing bare (unmodified) and modified electrodes. Results of these studies have recently been published in the *Journal of the Electrochemical Society*,[15] and reuse is permitted here under the Creative Commons Attribution 4.0 License (https://creativecommons.org/licenses/by/4.0/).

CHAPTER 2

EXPERIMENTAL

Materials

All chemicals were used as received from the manufacturer. Potassium ferricyanide and sodium borohydride were obtained from Fisher Scientific. Hexaaminеruthenium(III) chloride was acquired from Strem Chemicals. Potassium chloride, ferrocenemethanol and an aqueous solution of 20% (w/w) PDDA (average molecular weight range 200,000-350,000) were procured from Sigma Aldrich. L-glutathione and tetrachloroaurate(III) trihydrate were purchased from Alfa Aesar. Graphite ink (C2050106D7) and Ag/AgCl paste (C2051014P10) used for printing the electrodes were purchased from Gwent Electronic Materials Ltd in Pontypool, UK. All aqueous solutions were prepared with 18.2 MΩ.cm ultrapure water, which was obtained by passing deionized water through a Millipore Synergy purifier.

Preparation of SPCEs

Electrodes in these studies were prepared in-house by manual screen-printing through use of 200 mesh nylon screens and conductive graphite and Ag/AgCl pastes. The screen was coated with a diazo photo emulsion,[15] and allowed to dry overnight in the dark. Patterns of the working, counter and reference electrodes, contact pads, and conductive paths connecting electrodes to the contact pads (Figure 2) were designed using a computer graphics program (Macromedia Fireworks MX), and printed on acetate tracing paper using a desktop inkjet printer. The electrode design consisted of three 2 mm x 5 mm (width x length) graphitic contact pads connected to electrodes through 1 mm x 20 mm conductive paths. A circular 2 mm diameter carbon working electrode was designed to be at the end of the center conductive path between 2 mm wide arc-shaped carbon counter and Ag/AgCl reference electrodes (Figure 2).

The acetate paper patterns were positioned on top of the diazo photo emulsion-coated screen and under a piece of transparent glass (8 in x 10 in). The screen was then placed in a cabinet that was covered with a black paper on the inside, where it was exposed (for 7 minutes) to light from a 150 W clear incandescent bulb that was located 18 inches above the screen. This was to cure the coating on all parts of the screen except the electrode patterns. The uncured diazo photo emulsion that defined the electrodes, conducting paths, and contact pads was then flushed out using cold tap water, and the screen was air-dried.

Graphite ink was forced through the screen using a squeegee (Figure 1B) and transferred onto a polyimide or cellulose acetate film (Figure 2). This produced the working and counter electrodes, contact pads, and conductive paths that connect the electrodes to the contact pads. The printed ink was cured in an oven at a temperature of 60 ºC for 30 min. Afterwards, the reference electrode was also printed on top of the third conducting path by forcing Ag/AgCl ink through the screen onto the acetate sheet. Curing was again done in the oven at 60 ºC for 30 min.

Kapton tape was placed over conductive paths to provide insulation and help define working electrode area (Figure 2). A digital camera was used to obtain images of ten screen-printed electrodes so that the geometric surface areas of the working electrodes could be measured using ImageJ software.[22] The average geometric surface area of the electrodes was found to be 2.52 (±0.29) x 10^{-2} cm^2 (n = 10).

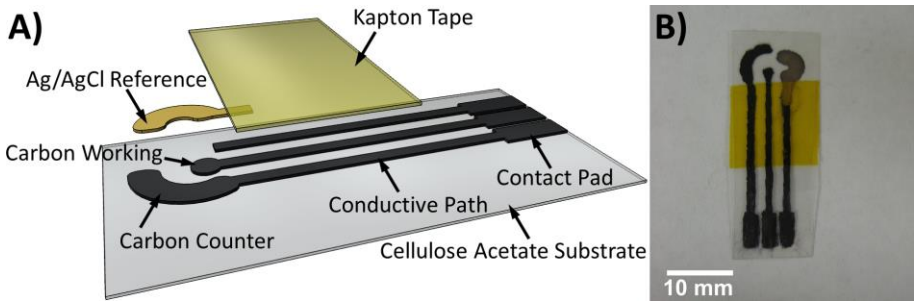

Figure 2: Images of screen-printed carbon electrodes. A) An illustrated exploded view design and B) photographic image of a screen-printed carbon electrode on cellulose acetate with conductive paths covered with yellow polyimide (Kapton) tape. Reproduced with permission from Reference 14.

Synthesis of Glutathione-Capped Gold Nanoparticles

Glutathione-capped gold nanoparticles (GSH-AuNPs) were synthesized based on a previous report.[10] In a fume hood, aqua regia (3 HCl: 1 HNO_3) was used to rinse glass vials and transfer pipettes to be used in the preparation. Glassware was then rinsed with copious amount of ultrapure water, and dried in an oven. A plastic spatula was used to transfer 19.7 mg of hydrogen tetrachloroaurate (III) trihydrate ($HAuCl_4 \cdot 3H_2O$) into one of the oven-dried vials, and 7.7 mg of L-glutathione was also added, followed by 3.5mL of a 14.4% (v/v) acetic acid and methanol mixture. In a fume hood, the resulting gold(III) chloride mixture was placed on a magnetic stirrer and mixed for 5 min. 30 mg of sodium borohydride ($NaBH_4$) was quickly dissolved in 1.5 mL ultrapure water and this solution was added dropwise to the gold solution while stirring, changing its color from bright yellow to brown immediately.

The mixture was stirred for 2 h, after which the suspension of glutathione-capped gold nanoparticles (GSH-AuNPs) was split equally into two 50 kDa MW cut-off filter centrifuge tubes. Centrifugation was carried out at 2150x*g* (where *g* is the standard acceleration due to gravity) for 8 min using a VWR Clinical 100 centrifuge. The liquid collected at the bottom the tube was discarded, and the GSH-AuNPs were resuspended in ultrapure water and centrifuged again. This process was repeated two more times after which the GSH-AuNPs were resuspended

in 20 mM HEPES buffer (pH 8). After centrifugation was completed, the supernatant was discarded, and GSH-AuNPs were resuspended in HEPES buffer. Centrifugation and resuspension was repeated four times until a clear supernatant solution was obtained. The GSH-AuNPs were finally resuspended in 1.5 mL HEPES buffer. The resuspended particles were diluted 10-fold using HEPES buffer, and a UV-vis spectrum was taken using a Shimadzu 1700 UV-vis spectrophotometer to estimate the size of the particles.[10,23]

Layer-by-Layer Modification of SPCEs

SPCEs are often pretreated to remove any adsorbed species and better expose conductive graphite particles.[24,41] In the present studies, SPCEs were pretreated according to a previous report.[32] SPCEs were placed in a solution of 0.5 M H_2SO_4, and a linear voltammetric sweep was performed from -1.2V to +1.5 V vs. Ag/AgCl using a CHI instruments potentiostat (CHI 400). The electrodes were then rinsed with ultrapure water and air-dried. This was followed by depositing the GSH-AuNPs on the SPCEs through LbL method as previously described.[10,25]

Using a micropipette, 2 µL of 2 mg/mL solution of PDDA in 50 mM sodium chloride was deposited onto the working electrode. After 20 min, the PDDA-modified electrode was rinsed with ultrapure water and dried using nitrogen gas. A micropipette was then used to deliver 2 µL of GSH-AuNP suspension onto the PDDA-modified working electrode. After 20 min, it was rinsed with ultrapure water to remove any excess or loosely bound GSH-AuNPs and dried with nitrogen gas.

Electrochemical Measurements

A computer-controlled CHI 400 electrochemical analyzer, operated in a potentiostatic mode, was used to carry out all electrochemical measurements. A solution of 0.1 M potassium chloride (KCl) containing a common redox probe, i.e. 1 mM potassium ferricyanide, 0.5 mM

ferrocenemethanol or 1 mM hexaaminеruthenium(III) chloride, was poured into a 10-mL beaker. A bare or modified SPCE was placed in the solution, and cyclic voltammetric (CV) measurements were then carried out at scan rates of 10-200 mV/s. Electrodes were rinsed with water between successive experiments with different redox probes. Currents measured for each redox probe were converted to current densities by normalizing by the geometric surface area of the individual electrode that was used for each experiment.

CHAPTER 3

RESULTS

Characterization of GSH-AuNPs

The size of the GSH-AuNPs was determined by UV-Vis spectrophotometry as previously described. [23] The UV-vis spectrum of the GSH-AuNPs gave a characteristic absorbance peak due to surface plasmon resonance[26] at 515 nm (λ_{SPR}) (Figure 4), indicating the particles to be less than 30 nm in diameter.[23,] Since absorbance at λ_{SPR} (A_{SPR}) is known to decrease in relation to absorbance at other wavelengths in a manner that is dependent on particle size, the diameter of AuNPs smaller than 35 nm can be estimated through the ratio of absorbance at 515 nm to absorbance at 450 nm (A_{SPR}/A_{450}) as described in a previous report.[23] The size of the particles was found to be 5 nm using this estimate. Though this estimate is based on a model developed from the match between theoretical absorbance of bare spherical gold nanoparticles and experimental absorbance data for citrate-capped gold nanoparticles,[23] it has been widely employed in literature[27] and at least one previous report showed no significant effect of capping agent on nanoparticle size for glutathione- and citrate-capped metal nanoparticles.[28] Most importantly, the 5 nm particle size estimated is in agreement with particles synthesized by the same protocol and characterized by UV-Vis spectroscopy and transmission electron microscopy (TEM) in a previous report.[25]

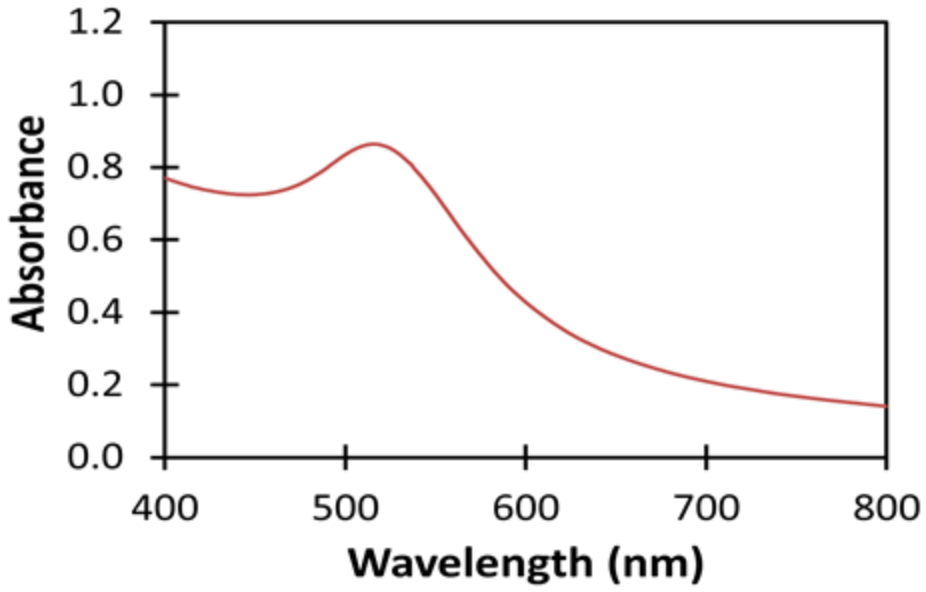

Figure 3: Absorption spectrum of GSH-AuNPs in 20 mM HEPES buffer (pH 8.0). Characteristic absorption peak is found at 515 nm.

Determination of Extent of Coverage of GSH-AuNPs

To directly estimate electroactive surface area of GSH-AuNPs incorporated on SPCEs, CVs of bare and modified SPCEs were obtained in 0.5 M H_2SO_4 (Figure 4). These CVs exhibited an anodic peak centered at +1.25 (± 0.010) V and cathodic peak at 0.66 (± 0.025) V vs. Ag/AgCl that were consistent with the oxidation of gold and reduction of gold oxide, respectively.[19,30] No noticeable peaks were observed on bare or PDDA-modified SPCEs. Complete oxidation of a monolayer of gold or reduction of gold oxide corresponds to a charge of 400 μC cm^{-2}.[29] The charge associated with the reduction peak of GSH-AuNPs was thus used to estimate the electroactive surface area that can be attributed to gold.[30] In this manner, the electroactive surface area provided by GSH-AuNPs on the GSH-AuNP/PDDA-modified SPCEs was found to be 1.69 (±0.34) x 10^{-2} cm^2. This surface area represents only 67 (±9) % of the geometric surface areas of the SPCEs, which suggests incomplete surface coverage of GSH-

AuNPs or incomplete electron transfer between GSH-AuNPs and the underlying SPCEs.

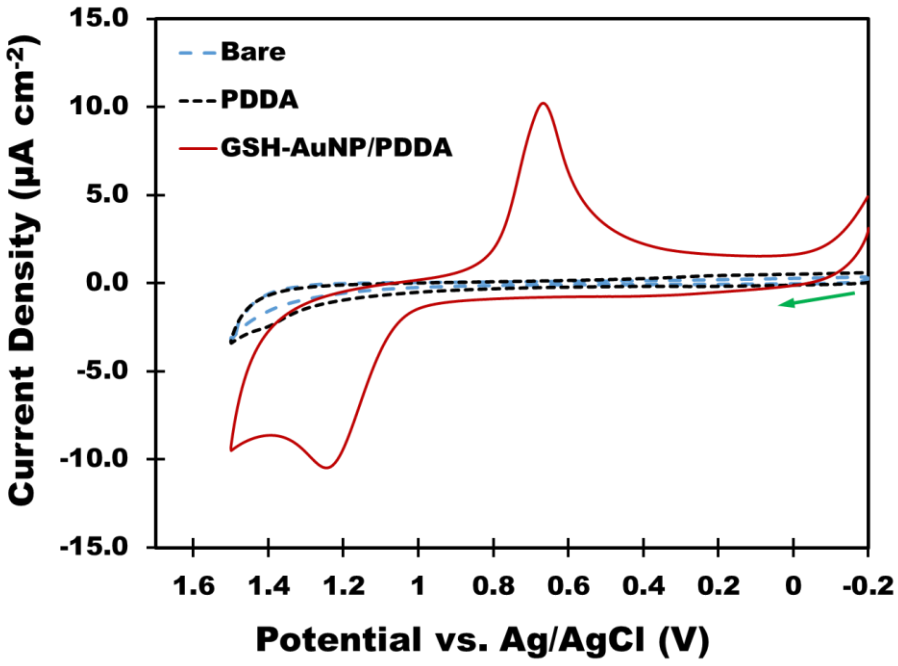

Figure 4*:* Representative CVs of bare (dashed blue line), PDDA-modified (dotted black line) and GSH-AuNP/PDDA-modified (solid red line) SPCEs in 0.5 M H_2SO_4. Arrow indicates direction of scan. Scan rate is 100 mV/s.

Cyclic Voltammetric Studies of Common Redox Probes Using Bare, PDDA- and GSH-AuNP/PDDA-Modified SPCEs

The electrochemical responses of bare, PDDA-modified and GSH-AuNP/PDDA-modified SPCEs were measured using three common redox probes to determine the effect of surface modification on electrochemical response. The $Fe(CN)_6^{3-/4}$ redox couple produced a pair of peaks centered at 0.1223 V vs. Ag/AgCl as expected (Figure 5).[15] Similar to a previous report,[10] GSH-AuNP/PDDA-modified SPCEs exhibited lager peak currents and smaller peak separations between cathodic and anodic peaks compared to the bare SPCEs. However, there was little difference between peak currents associated with the reduction of $Fe(CN)_6^{3-}$ using PDDA-modified and GSH-AuNP/PDDA-modified SPCEs. Interestingly, $Fe(CN)_6^{3-/4-}$ typically

produced a couple of extra peaks using PDDA-modified electrodes (Figure 5) that were not observed with either bare or GSH-AuNP/PDDA-modified SPCEs. These extra peaks were visible using 7 out of 10 PDDA-modified SPCEs, with the rest (3 out of 10 PDDA-modified SPCEs) not showing these additional peaks (Figure 6). Contrary to the responses of $Fe(CN)_6^{3-/4-}$, there were no significant differences in the responses of $Ru(NH_3)_6^{3+/2+}$ (Figure 7) or $FcCH_2OH$/ $FcCH_2OH^+$ (Figure 8) using bare and modified SPCEs.

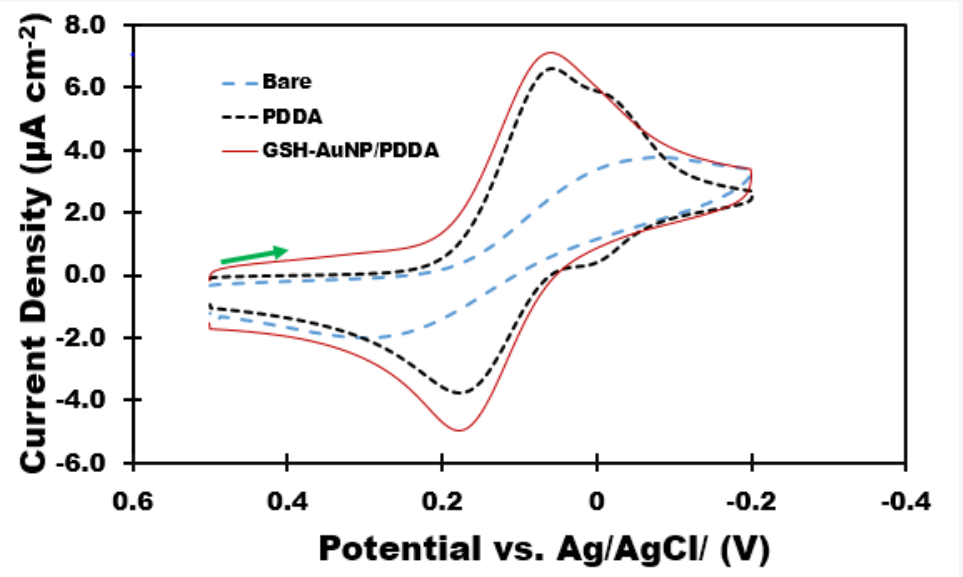

Figure 5: Representative CVs of 1 mM $Fe(CN)_6^{3-/4-}$ in 0.1 M KCl on bare, 7 out of 10 PDDA-, and GSH-AuNP/PDDA-modified SPCEs. Arrow indicates direction of forward scan. Scan rate = 100 mV/s.

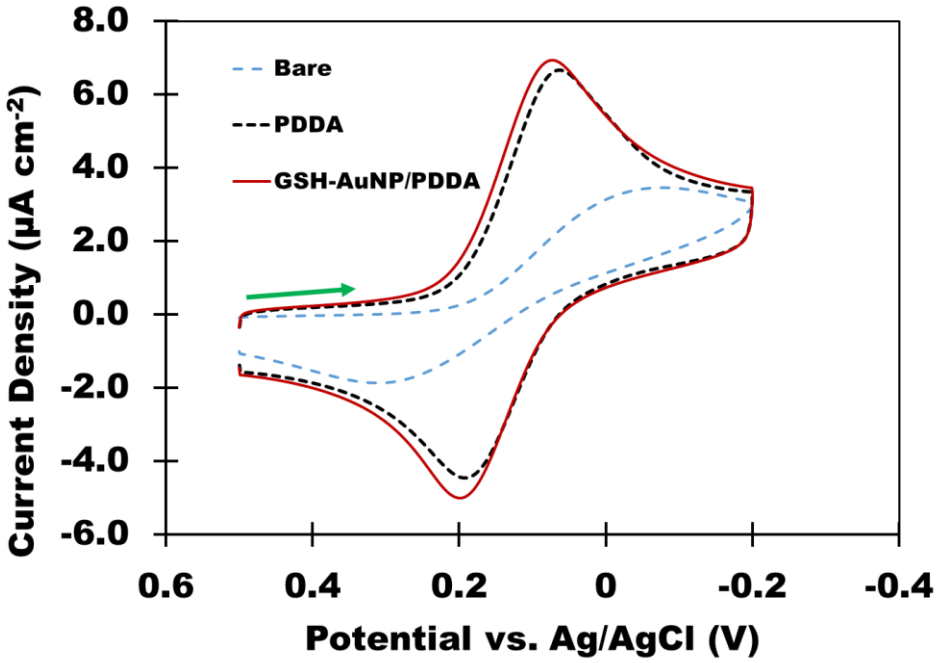

Figure 6: Representative CVs of 1 mM $Fe(CN)_6^{3-/4-}$ in 0.1 M KCl on bare, 3 out of 10 PDDA-, and GSH-AuNP/PDDA-modified SPCEs. Arrow indicates direction of forward scan. Scan rate = 100 mV/s.

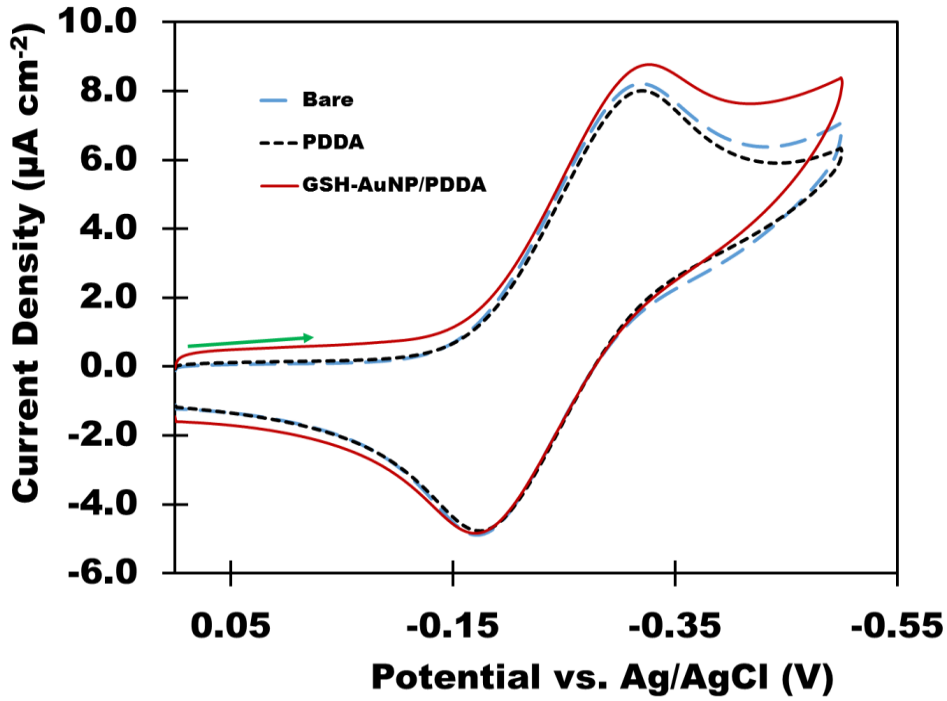

Figure 7: Representative CVs of 1 mM $Ru(NH_3)_6^{3+/2+}$ in 0.1 M KCl on bare, PDDA- and GSH-AuNP/PDDA-modified SPCEs. Arrow indicates direction of forward scan. Scan rate = 100 mV/s.

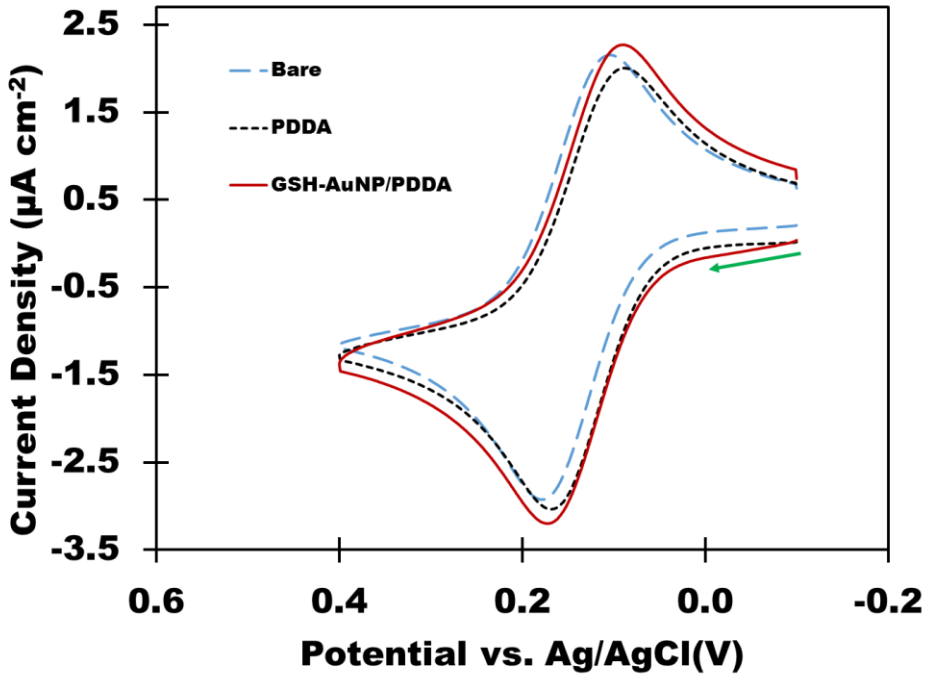

Figure 8: Representative CVs of 0.5 mM $FcCH_2OH$ in 0.1 M KCl on bare, PDDA-modified and GSH-AuNP/PDDA-modified SPCEs. Arrow indicates direction of forward scan. Scan rate= 100 mV/s.

As depicted in representative CVs (Figures 5-8), average peak current densities (Table 1) and peak-to-peak separations (Table 2) show that the only significant differences between electrochemical responses of bare and modified electrodes are found when $Fe(CN)_6^{3-}$ is used as the redox probe. CV responses of $Fe(CN)_6^{3-/4-}$ using bare SPCEs exhibited smaller average peak current density (138 µA cm^{-2}) and larger average peak separation (217 mV) compared to either PDDA- or GSH-AuNP/PDDA-modified SPCEs. There were no significant differences (95% confidence level) between average CV responses of $Fe(CN)_6^{3-/4-}$ using PDDA- and GSH-AuNP/PDDA-modified SPCEs, and no significant differences between bare and modified SPCEs using the other two redox probes. Overall, average peak current densities varied by up to 15% and average peak separations varied by as much as 27% among similarly prepared electrodes using each redox probe. These variations in current densities and peak separations as well as the

inconsistent extra peaks observed on PDDA-modified SPCEs with ferricyanide (Figures 5-6) may be due to the uneven distribution of conductive graphite particles in the polymeric binder or inconsistencies in the manual screen-printing process.

Table 1: Average peak current densities (j_p) of forward voltammetric scans of the redox probes each in 0.1 M KCl with the bare, PDDA- and GSH-AuNP/PDDA-modified SPCEs at a scan rate of 100 mV/s.

	j_p (μA cm^{-2}) for Various Redox Probes		
SPCE Modification	**1 mM $Fe(CN)_6^{3-}$**	**0.5 mM $FcCH_2OH$**	**1 mM $Ru(NH_3)_6^{3+}$**
None (Bare)	138 (± 18)	-126 (± 6)	214 (± 29)
PDDA	233 (± 22)	-129 (± 8)	215 (± 32)
GSH-AuNP/PDDA	213 (± 26)	-122 (± 13)	223 (± 23)

Table 2: Average peak-to-peak separations (ΔE_p) for the redox probes each in 0.1 M KCl with the bare, PDDA-modified and GSH-AuNP/PDDA-modified SPCEs at a scan rate of 100 mV/s.

	ΔE_p (mV) for Various Redox Couples		
SPCE Modification	**$Fe(CN)_6^{3-/4-}$**	**$FcCH_2OH/FcCH_2OH^+$**	**$Ru(NH_3)_6^{3+/2+}$**
None (Bare)	217 (± 49)	90 (± 17)	109 (± 29)
PDDA	133 (± 30)	94 (± 17)	113 (± 25)
AuNP/PDDA	136 (± 34)	102 (± 18)	117 (± 32)

Electroactive Surface Areas of SPCEs

Cyclic voltammetric (CV) data can be used to estimate electroactive surface area,[7,8,10,15] an important factor that helps determine electrode sensitivity as electrochemical signal involving

charge and current are proportional to electrode area. This estimation is typically done using Randles-Sevcik equation at 25 °C (eqn. 1).[7,8,10]

$$i_p = (2.69\times10^5)n^{3/2}AD^{1/2}Cv^{1/2} \quad (1)$$

Where A denotes the electroactive surface area (in cm^2), i_p is the peak current (in amperes), *n* is the number of electrons involved in the redox process, D represents the diffusion coefficient of the redox probe (in $cm^2\ s^{-1}$), C denotes the bulk concentration (in mol cm^{-3}) of the electroactive species, and v is the scan rate (in V s^{-1}). For these studies, D was taken to be 7.60 x 10^{-6} cm^2s^{-1} for $Fe(CN)_6^{3-}$, 8.43 x $10^{-6}cm^2s^{-1}$ for $Ru(NH_3)_6^{3+}$, and 7.80 x 10^{-6} cm^2s^{-1} for $FcCH_2OH$ based on literature values.[9,15]

Since the SPCEs exhibited peak-to-peak separations larger than 59 mV (Table 2), the modified version of Randles-Sevcik equation (eqn. 2) was used to estimate the electroactive surface area[7,8,15] for bare, PDDA-modified and GSH-AuNP/PDDA-modified SPCEs.

$$i_p = (2.69\times10^5)n^{3/2}AD^{1/2}Cv^{1/2}K(\Lambda,\alpha) \quad (2)$$

Where K*(*ʌ, α*)*, determined from a work of Matsuda and Ayabe,[31,32] is a function that depends on dimensionless parameters α, which is the electron transfer coefficient, taken to be 0.5 for the redox probes used in these studies,[9,33] and the rate parameter ʌ. The rate parameter ʌ is related to another parameter ψ (eqn. 3), which is determined from peak-to-peak separation values from CV measurements through Nicholson's work.[31,32]

$$\Lambda = \pi^{1/2}\psi \quad (3)$$

Using the CV results obtained with $Fe(CN)_6^{3-/4-}$, the average electroactive surface area calculated for the bare SPCEs was significantly smaller than the electroactive surface areas of the PDDA- and GSH-AuNP/PDDA-modified SPCEs (Table 3). The calculated average electroactive area of bare SPCEs was also smaller than the average geometric surface area of 2.52 (±0.29) x

10^{-2} cm^2. The presence of PDDA on the SPCEs caused a 61% increase in estimated electroactive surface area while the GSH-AuNP deposition resulted in a 54% increase in estimated surface area over the bare SPCEs according to measurements based on $Fe(CN)_6^{3-/4-}$. Though the electroactive surface areas of the bare SPCEs determined with the use of $Fe(CN)_6^{3-/4-}$ were different from the areas of the PDDA-and AuNP/PDDA-modified electrodes, the calculated surface areas of the PDDA- and AuNP/PDDA-modified SPCEs using $Fe(CN)_6^{3-/4-}$ were similar to one another, and to those obtained with $FcCH_2OH$/ $FcCH_2OH^+$ and $Ru(NH_3)_6^{3+/2+}$ redox couples. There were also no significant differences in the surface areas of bare and modified SPCEs when $FcCH_2OH/FcCH_2OH^+$ and $Ru(NH_3)_6^{3+/2+}$ redox couples were used (Table 3).

Table 3: Electroactive surface areas of bare, PDDA-modified and GSH-AuNP/PDDA-modified SPCEs with the various redox couples in 0.1 M KCl supporting electrolyte.

	A (cm^2) for Various Redox Couples		
SPCE	**1 mM**	**0.5 mM**	**1 mM**
Modification	**$Fe(CN)_6^{3/4-}$**	**$FcCH_2OH/FcCH_2OH^+$**	**$Ru(NH_3)_6^{3+/2+}$**
None(Bare)	$1.81(\pm0.44)x10^{-2}$	$2.81(\pm 0.35)\ x10^{-2}$	$2.81\ (\pm 0.49)\ x10^{-2}$
PDDA	$2.84(\pm0.44)x10^{-2}$	$2.87\ (\pm0.49)\ x10^{-2}$	$2.80(\pm 0.55)\ x10^{-2}$
AuNP/PDDA	$2.71(\pm0.37)x10^{-2}$	$2.79\ (\pm 0.49)\ x10^{-2}$	$2.71\ (\pm 0.50)\ x10^{-2}$

Determination of Roughness Factor of Bare SPCEs

Another measurement used to characterize SPCEs is the roughness factor (R_A),[7,15] which corresponds to the ratio of electroactive surface (A) area to the geometric surface area (A_{geo}) of the electrode (eqn. 4).

$$R_A = A/A_{geo} \quad (4)$$

Inks used for printing SPCEs contain conductive graphite particles and polymeric binder(s) dispersed in electrochemically inert solvents.[7,12] These binders (e.g. polyvinyl chloride (PVC), polyvinyl acetate (PVA), etc.)[7,12] are nonconductive or electrochemically inactive. As the name suggests, they serve as adhesives to hold the conductive graphite particles together at tunneling distances.[12,31] The relative amounts of these binding materials to the conductive particles in the ink can determine the electrochemical properties of the electrodes printed from the inks, as there are some parts of the electrodes that are electrochemically active while others are electrochemically inactive. Thus, the roughness factor can essentially be taken to be a measure of the "real" electroactive surface area of the electrodes.[7,33]

Converting these R_A values of the bare electrodes to percentages, the electroactive surface areas obtained from $FcCH_2OH$/ $FcCH_2OH^+$ and $Ru(NH_3)_6^{3+/2+}$ results gave very similar percent R_A values of 113 (±5)% and 110 (±10)%. The R_A value obtained for bare SPCEs from the $Fe(CN)_6^{3-/4-}$ results was significantly smaller than those determined from $FcCH_2OH$/ $FcCH_2OH^+$ and $Ru(NH_3)_6^{3+/2+}$ measurements. However, the R_A value of 71 (±10)%, for bare SPCEs calculated from the $Fe(CN)_6^{3-/4-}$ results falls within the 39-79% R_A values[7] reported for similar measurements for commercially available SPCEs using $Fe(CN)_6^{3-/4-}$.

Determination of Heterogenous Electron Transfer Rate Constants

The proportions of conductive graphitic particles and nonconductive polymeric binders in inks used in printing SPCEs can affect the rate at which electrons are transferred between electroactive samples and the electrodes.[7,33] Similar electrodes have been previously characterized by their heterogeneous electron transfer rate constants (k_0) using the Nicholson method (eqn. 5).[32]

$$k_0 = \psi(\pi D_O^{1-\alpha} D_R^{\alpha} n f v)^{1/2} \quad (5)$$

Where ψ represents the same kinetic parameter introduced in eqn. 3. Do and D_R are diffusion coefficients of oxidized and reduced species, respectively, while f corresponds to $\frac{F}{RT}$ where F (96485.333 C/mol), R (8.314 J $K^{-1}mol^{-1}$) and T (in K) are Faraday's constant, the Universal Gas Constant, and temperature, respectively. D_O values for $Fe(CN)_6^{3-}$ and $Ru(NH_3)_6^{3+}$ were the same as D values listed above that were used to calculate electroactive surface area, while D_R values for $Fe(CN)_6^{4-}$ and $Ru(NH_3)_6^{2+}$ were 6.5 x 10^{-6} cm^2 s^{-1} and 1.19 x 10^{-5} cm^2s^{-1}, respectively, based on literature.[25,34,35] For $FcCH_2OH$ and $FcCH_2OH^+$, Do = D_R = 7.80 x 10^{-6} cm^2s^{-1}.[7,9,35]

Using an ambient temperature of 25 ºC (298.15 K), Faraday's constant of 96,485C, and Universal Gas Constant of 8.314 J $K^{-1}mol^{-1}$ along with the stated D values, it was observed that neither the presence of PDDA nor GSH-AuNPs on the SPCEs seem to have influenced the electron transfer rate constants of $FcCH_2OH/FcCH_2OH^+$ and $Ru(NH_3)_6^{3+/2+}$, as no differences in rate constants were observed between the bare, PDDA-modified and GSH-AuNP/PDDA-modified SPCEs with the two redox probes. With $FcCH_2OH/FcCH_2OH^+$, the rate constant determined was 6.8 (±2.1) x 10^{-3} cm^2 s^{-1} while a value of 4.1 (±1.7) x10^{-3} cm^2 s^{-1} was obtained with $Ru(NH_3)_6^{3+/2+}$. The mean k_0 for $Fe(CN)_6^{3-/4-}$ for the modified SPCEs was 2.9 (±1.2) x 10^{-3} cm^2 s^{-1} while it was 1.2 (±0.25) x 10^{-3} cm^2 s^{-1} for the bare SPCEs. Electron transfer rate constant values ranging from 1.67x 10^{-5} to 8.3 x 10^{-3} cm^2 s^{-1} values have been reported for $Fe(CN)_6^{3-/4-}$ with other screen-printed carbon electrodes.[9,36]

CHAPTER 4

DISCUSSION

Nanoparticle-modified SPCEs have been extensively utilized as biosensing platforms.[2,10] The increase in electroactive surface area provided by the inclusion of nanomaterials on SPCE surfaces is often cited as an important factor in explaining the improvements in electrochemical responses that have been documented for nanoparticle-modified SPCEs compared to bare (unmodified) SPCEs.[10,37] For example, Chikkaveeraiah et al. recently reported that LbL modification of SPCEs using PDDA and 5 nm GSH-AuNPs leads to an improvement of 102% in electroactive surface area compared to that of the unmodified (bare) SPCEs.[10] These GSH-AuNP/PDDA-modified SPCEs have been employed in sandwich-type electrochemical immunoassays for various protein biomarkers related to prostate cancer and oral cancer.[10] One aspect of the design of GSH-AuNP/PDDA-modified SPCEs that has been used to help explain their success as sensing platforms is the large electroactive surface area provided by the inclusion of GSH-AuNPs, which leads to an increase in electrochemical response compared to unmodified SPCEs.[10] However, electroactive surface areas were determined through CV measurements of $Fe(CN)_6^{3-/4-}$ using bare and GSH-AuNP/PDDA-modified SPCEs.

Recent reports have documented $Fe(CN)_6^{3-/4-}$ response on other carbon-based electrodes and demonstrated that electrochemical signal enhancement typically attributed to increase in electroactive surface area is more likely the result of surface effects that are unrelated to electroactive surface area. For instance, cyclic voltammetric studies of $Fe(CN)_6^{3-/4-}$ with highly oriented pyrolytic graphite (HOPG) electrodes suggested that the redox probe was sensitive to electrode surface charges, resulting in poorer kinetics of the electron transfer process between the redox probe and electrodes.[20] Other studies with graphene nanoflake electrodes also reported the

dependence of electrochemical properties of $Fe(CN)_6^{3-/4-}$ on pH of the measuring environment and on electrolyte concentrations.[21]

The results of these current studies, similar to those reported for $Fe(CN)_6^{3-/4-}$ using HOPG and graphene-modified electrodes, suggest that caution must be exercised when interpreting CV responses of $Fe(CN)_6^{3-/4-}$ on SPCEs and their relationship to electroactive surface area. The studies carried out by Chikkaveeraiah et al.[10] seem to have overlooked the potential role of the PDDA layer underlying the 5 nm GSH-AuNPs, in enhancing the peak currents associated with ferricyanide, hence ended up associating the signal increase entirely with the GSH-AuNPs on the SPCEs.

In the current studies, the voltammetric responses of PDDA-modified and GSH-AuNP/PDDA-modified SPCEs with $Fe(CN)_6^{3-/4-}$ were very similar (Figures 5 and 6), indicating that the previously observed signal enhancement[10] documented between bare and GSH-AuNP/PDDA-modified SPCEs for this same system cannot be attributed to the presence of GSH-AuNPs as previously thought. The peaks for $Fe(CN)_6^{3-/4-}$ obtained using bare SPCEs were widely separated and exhibited low peak currents, while the modified SPCEs produced smaller peak-to-peak separations with higher peak currents. Large peak separations of $Fe(CN)_6^{3-/4-}$ have also been reported for commercially available bare SPCEs,[8] HOPG,[34] and graphene-modified [21] electrodes.

Voltammetric peak separations of $Fe(CN)_6^{3-/4-}$ using other gold and platinum SPEs have similarly been documented to be dependent on electrode surface structure.[38,39] For instance, large peak-to-peak separation values have been reported for $Fe(CN)_6^{3-/4-}$ on bulk screen-printed gold and platinum electrodes.[38,39] Upon electrodeposition of a layer of gold nanoparticles onto gold screen-printed electrodes, however, the peak separation for $Fe(CN)_6^{3-/4-}$ decreased from 300 mV

to 90 mV,[38] indicating that relative amounts of conductive particles and nonconductive polymeric binders in screen-printing inks may also play an important role in determining the electrochemical properties of screen-printed electrodes. The importance of relative amounts of ink contents have been demonstrated by using $Ru(NH_3)_6^{3+/2+}$ with SPCEs that were produced from customized graphite inks with varying graphite and binder compositions.[40] Electrodes prepared from inks having higher percentages of conductive graphite particles exhibited smaller peak-to-peak separations than those made from inks with lower percentages of the conductive particles distributed in large amounts of polymeric binders.[40]

In addition to modification with nanoparticles, electrochemical properties of SPCEs can also reportedly be improved by treating the electrode surface with organic solvents like N,N-dimethyl formamide (DMF) [18] or mechanical polishing.[24] For example, treatment of SPCEs with DMF reportedly resulted in enhancing the electroactive surface area by 57-fold compared to the geometric surface area of the electrodes when CV measurements were based on $Fe(CN)_6^{3-/4-}$ response.[35] Interestingly, more modest increases in electroactive surface areas ($\leq$ 1.38-fold) have been documented for similarly treated SPCEs when CV measurements were based on $Ru(NH_3)_6^{3+/2+}$, capasaicin, and dihydronicotinamide adenine nucleotide.[41] Also, peak currents of $Fe(CN)_6^{3-/4-}$ were reportedly increased by 8x for SPCEs that were polished with an agate lapping hammer.[35] However, in a similar study using $Ru(NH_3)_6^{3+/2+}$, polishing of the SPCEs with alumina had no significant effect on the electroactive surface area of the SPCEs, but the electrochemical activity of the electrodes toward nitrite was improved by two-fold.[35] These results indicate that electrochemical response of $Fe(CN)_6^{3-/4-}$ is influenced by electrode surface characteristics that are unrelated to electroactive surface area.

In the current studies, there are no significant differences in the voltammetric responses of the bare, PDDA-modified and GSH-AuNP/PDDA-modified SPCEs for the $Ru(NH_3)_6^{3+/2+}$ or $FcCH_2OH/FcCH_2OH^+$ redox couples (Figures 7 and 8). With each of the three redox probes used in these studies, PDDA-modified SPCEs exhibited peak currents that were similar to those obtained with the GSH-AuNP/PDDA-modified electrodes. However, PDDA-modified SPCEs typically exhibited extra pre-oxidation and post-reduction peaks for the $Fe(CN)_6^{3-/4-}$ redox couple that were absent when the bare or GSH-AuNP/PDDA-modified electrodes were used (Figure 5). Similar secondary waves have been reported for PDDA-modified glassy carbon electrodes[42] with the $Fe(CN)_6^{3-/4-}$ system, and have been attributed to the $Fe(CN)_6^{3-/4-}$ species that are trapped in the polymer on the electrode surface, forming species that are reduced or oxidized at slightly different potentials compared to $Fe(CN)_6^{3-/4-}$ that freely diffuses to the electrode surface.[42]

Even though CVs for GSH-AuNP/PDDA-modified SPCEs in 0.5 M H_2SO_4 confirmed the presence of the nanoparticles on the electrodes, the electroactive surface area attributable to the presence of the gold particles on electrodes was smaller than the geometric surface areas of the bare SPCEs. The electroactive gold surface area was also smaller than the electroactive surface areas of GSH-AuNP/PDDA-modified electrodes determined using the three redox probes. This finding directly challenges the previous assertion[10] that presence of the GSH-AuNPs on SPCEs resulted in the perceived 102% enhancement in electroactive surface area of the electrodes compared to the bare SPCEs.

Ultimately, the results of these studies suggest that LbL modification of SPCEs with GSH-AuNPs through the use of PDDA does not result in an increase in the electroactive surface area of the electrodes as previously reported.[10] The studies indicate that the electroactive surface

areas of bare, PDDA-modified and GSH-AuNP/PDDA-modified SPCEs were indistinguishable. Though previous reports that attribute the increase in $Fe(CN)_6^{3-/4-}$ response using nanoparticle-modified SPCEs over bare SPCEs to an increase in surface area provided by the presence of GSH-AuNPs on the electrode surface, the increase in electrochemical response of the $Fe(CN)_6^{3-/4-}$ redox couple instead appears to result from the sensitivity to chemical surface functionalities and charges that lead to lower electrochemical response of this particular redox probe on bare SPCEs. These findings seem to be consistent with similar determinations made for HOPG and graphene-modified electrodes with the ferricyanide redox couple.[21,40]

Conclusions

Caution must be exercised when evaluating the electrochemical benefits of the nanomaterials incorporated onto the surface of SPCEs through the use of voltammetric responses of $Fe(CN)_6^{3-/4-}$ as is typically done. Though the LbL technique is a simple, fast, and cost-effective way to prepare nanostructured SPCEs, the similarities between voltammetric responses of common redox probes on PDDA- and GSH-AuNP/PDDA-modified SPCEs suggest that the perceived increase in electroactive surface area, previously attributed to the GSH-AuNPs on the electrodes, may be more appropriately assigned to the possible role of PDDA in attracting more electroactive $Fe(CN)_6^{3-/4-}$ species onto electrode surface leading to an enhanced electron transfer between the redox probe and electrode. Even though the results of these studies indicate that the nanoparticles provided no enhancement in the electroactive surface areas of the SPCEs for this particular system and thus are not expected to provide general signal enhancement for other electrochemical species involved in sensing strategies, nanoparticles can provide other benefits.

Nanomaterials like gold nanoparticles can help control surface functionalities of the electrodes and provide sites for modification of the surface with desirable biomolecules or other

species. They can provide sites for immobilizing antibodies necessary for biosensing, and they can help catalyze redox reactions for some analytes as well.[43] The studies completed here help provide a more complete description of the role of GSH-AuNPs and PDDA in observed electrochemical response for these particular LbL-modified SPCEs. In addition to the specific system investigated here, this work may provide a framework for determining the effects of nanomaterial modification on electrochemical response for other modified electrodes. Since many nanomaterial-modified electrodes are characterized primarily or solely through CV measurements with $Fe(CN)_6^{3-/4-}$, these results should encourage more thorough characterization of nanostructured electrodes, which will hopefully lead to more informed design of electrochemical sensors.

Future Work

As a follow up to these studies, other potential roles of the gold nanoparticles on electrochemical properties of LbL SPCEs will be determined. Potential benefits of other nanomaterials or combinations of other nanomaterials with GSH-AuNPs in enhancing the electrochemical properties of SPCEs will also be explored. Ultimately, the modified electrodes will be used for measurements of proteins and DNA related to disease state of patients.

REFERENCES

1) Ngoepe, M.; Choonara, Y. E.; Tyagi, C.; Tomar, L.K.; du Toit, L.C.; Kumar, P.; Ndesendo, V. M.K.; and Pillay, V. Integration of biosensors and drug delivery technologies for early detection and chronic management of illness. *Sensors* **2013**, 13, 7680-7723.

2) Wang, J. Electrochemical biosensors: Towards point-of-care cancer diagnostics. *Biosens. Bioelectr.* **2006**, 21, 1887-1892.

3) Strimbu, K.; and Tavel, J.A. What are biomarkers? *Current opinion in HIV and AIDS*, **2010**, 5, 463-466.

4) Wallis, R.S.; Pai, M.; Menzies, D.; Doherty, T.M.; Walzl, G.; Perkins, M.D.; and Zumla, A. Biomarkers and diagnostics for tuberculosis: Progress, needs and translation into practice. *Lance*t **2010**, 375, 1920-1937.

5) Wisitsoraat, A.; Pakapongpan, S.; Sriprachuabwong, C.; Phokharatkul, D. Sritongkham, P. Lomas, T.; and Tuantranont, A. Graphene-PEDOT: PSS on screen printed carbon electrode for enzymatic biosensing. *J. Electroanal. Chem.* **2013**, 704, 208-213.

6) Grieshaber, D.; Mackenzie, R.; Voros, J.; and Reimhult, E. Electrochemical biosensors-sensor principles and architectures. *Sensors* **2008**, 8, 1400-1458.

7) So, M.; Hvastkovs, E.G.; Schenkman, J.B.; and Rusling, J.F. Electrochemiluminescent/voltammetric toxicity screening sensor using enzyme-generated DNA damage. *Biosens. Bioelectron.* **2007**, 23, 492-498.

8) Fanjul-Bolado, P.; Hernandez-Santos, D.; Lamas-Ardisana, P.J.; Martin-Pernia, A.; Costa-Garc, A. Electrochmical characterization of screen-printed and conventional carbon paste electrodes. *Electrochim. Acta* **2008**, 53, 3635-3642.

9) Kadara, R.O.; Jenkinson, N.; Banks, C.E. Characterization of commercially available electrochemical sensing platforms. *Sens. and Actuat. B* **2009**, 138, 556-562.

10) Chikkaveeraiah, V.B.; Mani, V.; Patel, V.; Gutkind, J.S.; and Rusling, J.F. Microfluidic electrochemical immunoarray for ultrasensitive detection of two cancer biomarker proteins in serum. *Biosens. Bioelectron.* **2011,** 26, 4477– 4483.

11) Meng Li, Yuan-Ting Li, Da-Wei Li, Yi-Tao Long. Recent developments and applications of screen-printed electrodes in environmental assays. *Analytica Chimica Acta*. **2012**, 734, 31–44.

12) Fletcher. S. Electrochemistry of carbon electrodes. In *Advances in electrochemical science and engineering*, 1st ed.; Alkire, R.C.; Bartlett, P.N.; Lipkowski, J., Eds.; Wiley-VCH Verlag GmbH & Co. KGaA: Weinheim, **2005**, Vol. 16; pp 425-443.

13) Drummond, T.G.; Hill, M.G.; and Barton, J.K. Electrochemical DNA sensors. *Nat. Biotech.* **2003**, 21, 1192.

14) Jin C.; Wei-de Z.; Jian-Shan Y. Nonenzymatic electrochemical glucose sensor based on MnO_2/MWNTs nanocomposite. *Electrochem. Commun.* **2008**, 10, 1268-1271.

15) Bishop, G.W.; Ahiadu, B.K.; Smith, J.L.; and Patterson, J.D. Use of redox probes for characterization of layer-by-layer gold nanoparticle-modified screen-printed carbon electrodes. *J. Electrochem. Soc.* **2017**, 164 B23-B28.

16) Hayat, A.; and Marty, J.L. Disposable screen-printed electrochemical sensors: Tools for environmental monitoring. *Sensors* **2014**, 10432-10453.

17) Manzanares-Palenzuela, C.L.; Fernandes, E.G.R.; Lobo-Castanon, M.J.; Lopez-Ruiz, B.; Zucolotto, V. Impedance sensing of DNA hybridization onto nanostructured phthalocyanine-modified electrodes. *Electrochim. Acta* **2016**, 221, 86- 95.

18) Sun, L.; Lu, Y.; Pan, Z.; Wu, T.; Liu, X.; Bao, N.; Yu, C.; He, H.; and Gu, H. Layer-by-layer assembly of hemoglobin-coated microspheres for enhancing the oxygen carrying capacity. *RSC Adv.* **2016**, 6, 59984-59987.

19) Alexeyeva, N.; and Tammeveski, K. Electroreduction of oxygen on gold nanoparticle/PDDA-MWCNT nanocomposites in acid solution. *Anal. Chim. Acta* **2008**, 618, 140-146.

20) Patel, A.N.; Collignon, M.G.; O'Connell, M.A.; Hung, W.O.Y.; McKelvey, K.; Macpherson, J. V.; and Unwin, P.R. A new view of electrochemistry at highly oriented pyrolytic graphite. *J. Am. Chem. Soc*. **2012**, 134, 20113-20130.

21) Lounasvuori, M.M.; Rosillo-Lopez, M.; Salzmann, C.G.; Caruana, D.J.; Holt, K.B. The influence of acidic edge groups on the electrochemical performance of graphene nanoflakes. *J. Electroanal. Chem.* **2015,** 753, 28-34.

22) Schneider, C.A.; Rasband, W.S.; and Eliceiri, K.W. NIH image to ImageJ: 25 years of image analysis. *Nat. Methods* **2012**, 9, 671-675.

23) Haiss, W.; Thanh, N.T.K.; Aveyard, J.; and Fernig, D.G. Determination of size and concentration of gold nanoparticles from UV-Vis spectra. *Anal. Chem.* **2007**, 79, 4215-4221.

24) Yan, M.; Zang, D.; Ge, S.; Ge, L.; and Yu, J. A disposable electrochemical immunosensor based on carbon screen-printed electrodes for the detection of prostate specific antigen. *Biosens. Bioelectron.* **2012**, 38, 355-361.

25) Mani, V.; Chikkaveeraiah, B.V.; Patel, V.; Gutkind, J.S. and Rusling, J. F. Ultrasensitive immunosensor for cancer biomarker proteins using gold nanoparticle film electrodes and multienzyme-particle amplification. *ACS Nano.* **2009**, 3, 585-594.

26) Link, S.; and El-Sayed, M.A. Shape and size dependence of radiative, non-radiative and photothermal properties of gold nanocrystals. *Int. Rev. in Phys. Chem*. **2000**, 19, 409-453.

27) Chandran, P.V.; Naseer M.; Udupa, N.; and Sandhyarani, N. Size controlled synthesis of biocompatible gold nanoparticles and their activity in the oxidation of NADH. *Nanotech*. **2012**, 015602.

28) Vinluan, R.D.; Liu, J.; Zhou, C.; Yu, M.' Yang, S.; Kumar A.; Zheng, J. Glutathione-coated luminescent gold nanoparticles: A surface ligand for minimizing serum protein adsorption. *ACS App. Mater. and Interf*. **2014**, 6, 11829-11833.

29) Trasatti S.; and Petrii, O. A. Real surface area measurements in electrochemistry. *Pure Appl. Chem.* **1991**, 63, 711-734.

30) Adams, K.L.; Jena, B.K.; Percival, S.J.; Zhang, B. Highly sensitive detection of exocytotic dopamine release using a gold-nanoparticle-network microelectrode. *Anal. Chem*. **2011**, 83, 920-927.

31) Eggings. B.R. *Chemical sensors and biosensors*. John Wiley and Sons Ltd.: Chichester, **2002**, pp 1-300.

32) Morrin, A.; Killard, A.J.; and Smyth, M.R. Electrochemical characterization of commercial and home-made screen-printed carbon electrodes. *Anal. Lett*. **2003,** 36, 2021-2039.

33) Cumba, L.R.; Foster, C.W.; Brownson, D.A.C.; Smith, J.P.; Iniesta, J.; Thakur, B.; do Carmo, D.R.; and Banks, C.E. Can the mechanical activation (polishing) screen-printed electrodes enhance their electroanalytical response? *Analyst* **2016**, 141, 2791-2799.

34) Bard A.J.; and Faulkner, L.R. *Electrochemical methods: Fundamentals and applications*, 2nd ed., John Wiley and Sons Inc.: New York **2001**, p 242.

35) Wang, Y.; Limon-Petersen, J. G.; and Compton, R. G. Measurement of diffusion coefficients of $[Ru(NH_3)_6]^{3+}$ and $[Ru(NH_3)_6]^{2+}$ in aqueous solution using microelectrode double potential step chronoamperometry. *J. Electroanal. Chem*. **2011,** 652, 13-17.

36) Randviir, E.P.; Brownson, D.A.C., Metters, J.P.; Kadara, R.O.; and Banks, C.E. The fabrication, characterization and electrochemical investigation of screen-printed graphene electrodes. *Phys. Chem. Chem. Phys*. **2014**, 16, 4598.

37) Ruzgas, T.; and Dock, E. Screen-printed carbon electrodes modified with cellobiose dehydrogenase: Amplification factor for catechol vs. reversibility of ferricyanide. *Electroanal*. **2003**, 15, 5-6.

38) Krejci, J.; Sajdlova, Z.; Nedela, V.; Flodrova, E.; Sejnohova, R.; Vranova, H.; and Plicka, R. Effective surface area of electrochemical sensors. *J. Electrochem. Soc*. **2014**, 161, B147-B150.

39) Erlenkötter, A.; Kottbus, M.; and Chemnitius, G.C. Flexible amperometric transducers for biosensors based on a screen-printed three electrode system. *J. Electroanal. Chem.* **2000**, 481,1, 82-94.

40) Choudry, A.N.; Kampouris, D.K.; Kadara, R.O.; and Banks, C.E. Disposable highly ordered pyrolytic graphite-like electrodes: Tailoring the electrochemical reactivity of screen-printed electrodes. *Electrochem. Commun*. **2010**, 12, 6-9.

41) Blanco, E.; Foster, C. W.; Cumba, L. R.; do Carmo, D. R.; and Banks, C. E. Can solvent induced surface modifications applied to screen-printed platforms enhance their electroanalytical performance? *Analyst* **2016**, 141, 2783-2790.

42) Maizels, M.; Heineman, W. R.; and Seliskar, C. J. Graphite electrodes coated with poly(dimethyldiallylammonium) chloride network films cross-linked by gamma-irradiation. *Electroanalysis* **2000,** 12, 4, 241-247.

43) Perez-Lopez, B. and Merkoci, A. Nanomaterial based biosensors for food analysis applications. *Trends in Food Sc. and Tech.* **2011**, 22, 625-639.

VITA

BEN KWASI AHIADU

Education: MS Chemistry, East Tennessee State University, Johnson City, TN, 2017
B. Sc. Chemistry, University of Cape Coast, Ghana, 2013
Akatsi College of Education, Ghana, 2006

Teaching Experience: Graduate Teaching Assistant, East Tennessee State University, Johnson City, TN (2016-2017)
Chemistry Teacher, Assin North Senior High School, Ghana (2013-2015)
Integrated Science Teacher, Toh-Kpalime L.A. J.H.S. (2006-2009)

Research Experience: Graduate research student, East Tennessee State University, 2015-2017 (Mentor: Dr. Gregory W. Bishop)

Prepared screen-printed electrodes through manual screen-printing of conductive inks.

Synthesized and characterized glutathione-capped gold nanoparticles (GSH-AuNPs).

Determined the role of GSH-AuNPs in voltammetric signal enhancement on layer-by-layer nano-structured screen-printed carbon electrodes.

Synthesized $[Ru(bpy)_3]^{2+}$ particles for chemiluminescence studies.

Undergraduate research student, University of Cape Coast, Ghana, 2012-2013 (Supervisor: Dr. Atsu V.Y. Barku)

Determined the phytochemical constituents and antioxidant properties of Mallotus oppositifolius.

Presentations: Ben K. Ahiadu, Jordan Smith, Jeremy Patterson, and Gregory W. Bishop. Role of Nanoparticles in Voltammetric Signal Enhancement Exhibited by Layer-by-Layer Gold Nanoparticle-Modified SPCEs, 68th South East Regional Meeting of the American Chemical Society, Columbia, SC., 2016, (10/24/2016, Oral Presentation, SERMACS 205).

Ben K. Ahiadu, Jordan Smith, Jeremy Patterson, and Gregory W. Bishop. Role of Nanoparticles in voltammetric signal enhancement exhibited by

layer-by-layer gold nanoparticle-modified SPCEs, (03/17/2017) Graduate seminar, ETSU.

Publications:

Gregory W. Bishop, Ben K. Ahiadu, Jordan Smith, and Jeremy Patterson. Use of redox probes for characterization of layer-by-layer gold nanoparticle-modified screen-printed carbon electrodes, *J. Electrochem. Soc.* **2017**, 164, B23-B28.

Barku, V.Y.A., Ahiadu, B.K.; and Abban, G. Phytochemical studies and antioxidant properties of the methanolic and aqueous extracts of the leaves of Mallotus oppositifolius. *J. Basic Applied Sci*. **2013**, 1, 20-30.

Honors and Awards:

Outstanding Graduate Student Award, Department of Chemistry, East Tennessee State University, Johnson City, TN (November 2016)